Mo bi-layer for thin film photovoltaic revisited

P.M.P. Salomé[1,*] , J. Malaquias[1,a], P.A. Fernandes[1,2,b] and A.F. da Cunha[1,c]

[1] I3N and Departamento de Física, Universidade de Aveiro, Campus Universitário de Santiago, 3810-193 Aveiro, Portugal

[2] Departamento de Física, Instituto Superior de Engenharia do Porto, Instituto Politécnico do Porto, Rua Dr. António Bernardino de Almeida, 431, 4200-072 Porto, Portugal

[*] Corresponding author, psalome@ua.pt

[a] jmalaquias@ua.pt

[b] pafernandes@ua.pt

[c] antonio.cunha@ua.pt

Abstract:

Thin film solar cells based in $Cu(In,Ga)Se_2$ as absorber layer use as back contact Mo. This metal is widely used in research and in industry but despite this, there is only a small number of published studies on the Mo properties. Properties such as low resistivity and good adhesion to soda lime glass (SLG) are hard to obtain at the same time. These properties are dependent on the deposition conditions and are associated with the overall stress state of the film. In this report, a study of the deposition of a Mo bi-layer is done by analysing firstly single and then bi-layers. The best bi-layer's properties was achieved when the bottom layer was deposited at $10x10^{-3}$ mbar with a thickness of 500 nm and the top layer deposited at $1x10^{-3}$ mbar with a thickness of 300 nm. Films deposited under these conditions showed good adhesion and a sheet resistivity lower than 0.8 Ω□.

Keywords: Mo, molybdenum, solar cells, thin films, electrical contact, bi-layer.

PACS:

Submitted to: Journal of Physics D: Applied Physics

1. Introduction

Thin film photovoltaics (PV) is an emerging worldwide industry. Due to the recent raise in energy prices and with more ecologic global concerns, PV has increasingly become a more important technology.

From all the current PV technologies, the one that is showing more industrial interest is the Cu(In,Ga)Se2 (CIGS) based photovoltaics. Several authors [1,2] believe that in the next decade, solar modules made from CIGS will overtake the giga Watt per year production. This type of technology is usually known as thin film PV, because, when compared with Si, the absorber layer is much thinner.

CIGS thin film solar cells are based on a layered structure represented in figure 1. Each one of the layers has a different role in working cells. The work presented in this report refers to the back contact layer. This layer has one main purpose which is basically to make the positive electrical contact of the cell. Although that is the main purpose, there are a few other requirements for this layer that need to be fulfilled, these are: have low resistivity; have good adhesion to soda lime glass (SLG); have low roughness; be chemically inert with the materials deposited on top, mainly Cu, In and Ga and Se; be stable during the high growth temperatures of the CIGS; allow Na diffusion from SLG since the properties of the CIGS films are influenced by the Na doping that occurs during growth, this has a positive effect in the solar cells performance [3]; have a high reflectance in the visible spectrum; have a temperature expansion coefficient similar to SLG and CIGS and form an ohmic contact with CIGS.

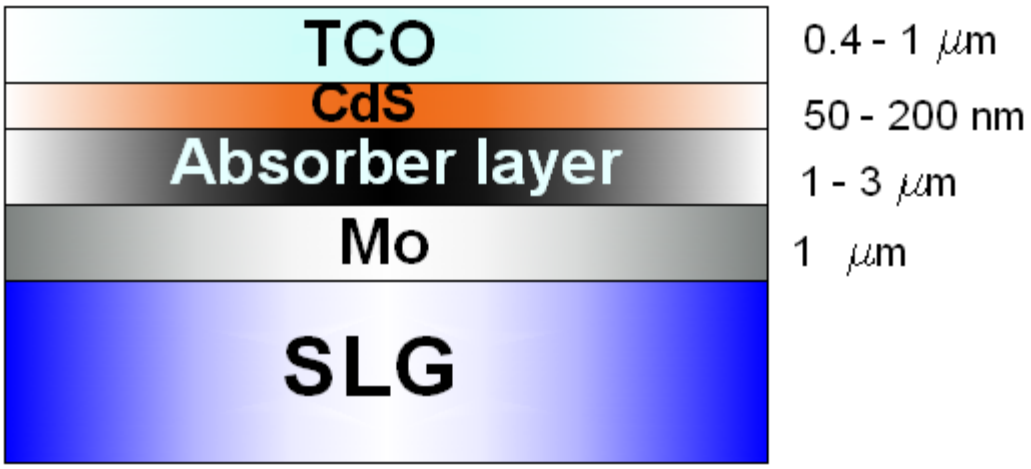

Figure 1. Layer sequence of a CIGS solar cell device, SLG stands for soda lime glass and TCO for transparent conductive oxide. The figure is not at scale.

One material that suits almost all those requirements is molybdenum (Mo). Mo is used by a large number of research groups and by the CIGS industry already in the market as it is shown in table 1. As comparison, it is also shown the CIGS growth method and the substrate. Despite

different methods and substrates used in all these companies, Mo as back contact is common to all of them. Mo is a metal which can be deposited as thin films with a good resistivity, a good adhesion and fairly smooth. It does not react with Cu, Ga or In and although it reacts with Se forming a $MoSe_2$ [4] layer there are small positive consequences for the solar cell performances reported [5]. Mo is also able to allow diffusion of Na [3] during CIGS growth, and it withstands its growth conditions.

Table 1: Substrates, CIGS growth methods and back contact material for several CIGS companies [6].

Company	Substrate	Back Contact	Growth CIGS Process
Shell Solar	Glass	Mo	Sputter/Selenization
Global Solar	Steel	Mo	Coevaporation
Miasole	Glass	Mo	Sputter/Selenization
Würth Solar	Glass	Mo	Coevaporation
Avancis	Glass	Mo	Sputter/RTP
Daystar Tech	Glass	Mo	Sputter
EPV	Glass	Mo	Sputter/evaporation
Ascent Solar	Polymer	Mo	Coevaporation
ISET	Glass/Flex	Mo	Ink/Selenization
Nanosolar	Flexible	Mo	Nanoink print/ RTP
Heliovolt	Glass	Mo	FASST
SoloPower	Steel	Mo	ED/RTP

One weak point that is usually acknowledged in using Mo, is its low reflectance in the visible part of the spectrum. Some groups [7] are trying to lower the thickness of the CIGS, their motivation is to make PV modules cheaper by using lower quantities of material. With smaller thickness in the absorber layer, the amount of light absorbed will decrease and therefore a good reflectance of light in the back contact is required. The basic idea is to increase the number of absorbed photons by reflecting those that are not absorbed, in the first passage, by the absorber. Other metals with low resistivity and reflectivity values, for example Pt, or Au, usually diffuse into the CIGS layer during the deposition [8]. Other reports have confirmed that cells made with Mo perform better than cells with a back layer with better reflectivity than Mo [8].

Mo is usually deposited by sputtering, mainly because these methods are used in industry and are easy to work with. Although Mo appears to be a good material to be used as back contact, its deposition is not without problems. When depositing Mo by these methods, the resistivity and the adhesion of the films are opposite effects making it difficult to have a film with both properties maximized. The reason why this happens is usually attributed to the film stress [9,10] state. Films that are deposited under compressive stress have low resistivity but also they have low adhesion. On the other hand, films that are deposited under tensile stress have good adhesion but high

resistivity. To overcome this problem Scofield *et al* [10] suggested depositing a bi-layer. If we can have a first layer with good adhesion followed by a layer with good resistivity, it might be possible to have a layer in which both properties would be adequate.

Despite the fact that the properties of Mo are well known and several groups already use, for a long time, a Mo-bilayer, the clear deposition conditions of such a layer have not been reported so far. Therefore the objective of this work is not to study all the referred properties but to present suitable deposition conditions of a Mo bi-layer. So, from the listed requirements, only the study of the properties that can be changed by the deposition method will be done. The properties that are required to make suitable Mo films are: thicknesses no bigger than 1000 nm; sheet resistances lower than 1 Ω□; good adhesion and being able to support temperatures up to 580 ºC and maintain the same properties as before.

1.1 Influence of the sputtering pressure

Sputtering working pressure influences the properties of sputtered atoms mainly by two ways [11,12]. The first is by changing the deposition rate and the second is the mean free path. With more pressure in the chamber the probability of a sputtered atom colliding with an Ar atom increases and thus changing the energy of the sputtered atoms. The energy with which the sputtered atoms arrive at the substrate is an important factor that determines the stress state of the films.

When sputtering at low pressures, Mo films have the tendency to become tightly packed, this tends to form films with a compressive stress and there is a decrease in resistivity. On the other hand, when sputtering at high pressures Mo films have a more porous columnar grain growth causing intergranular voids. This happens due to the reduced energy of sputtered atoms that arrive at the substrate. In terms of film properties, these voids make the resistivity higher but since there is not a reorganization of the arriving atoms, the adhesion is good. The tensile forces between these grains are attractive and inversely proportional in strength to the intergranular spacing [9]. Although these two explanations seem to be followed by different groups, there is an effect that is not fully explained yet. It is reported that Mo films have a maximum value in tensile stress and with increasing deposition pressure the tensile stress lowers and even gets to compressive stress. This effect is not explained so far.

The stress state of the films is then dependent on the microstructure of the Mo films which is also related with the deposition conditions. In ideal situations we would require to have the electrical behaviour of the compact films deposited at low pressures with compressive stress and the good adhesion that films with columnar grains show when they are in a tensile stress deposited

at high pressures. The stress state of the films studied in this work will be estimated using the rocking curve method.

1.2. The Rocking Curve method

The rocking curve method is a non destructive x-ray based method that allows us to estimate the stress state of a thin film. It is a complex technique that explores the strain done by a stress produced in the film. Let us consider that $\varepsilon_{\Phi,\psi}$ is the elastic lattice strain in a direction defined by the Euler angles ϕ and ψ with respect to the specimen frame of reference, see Figure 2.

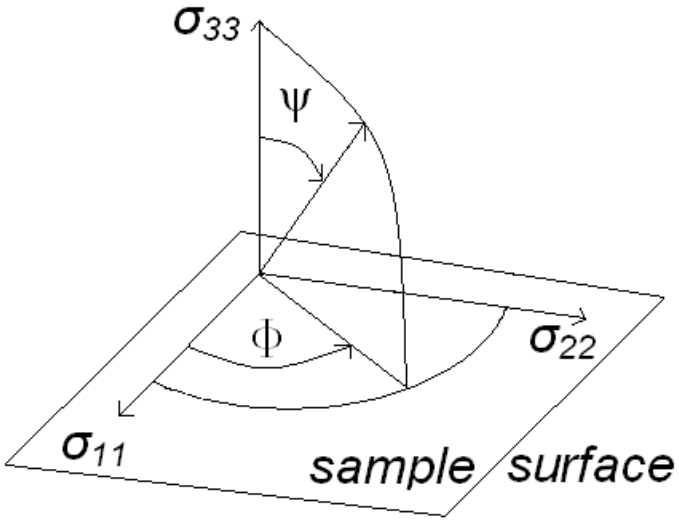

Figure 2. Definition of Euler angles ψ and ϕ with respect to the overall stress state.

The strain depends on the components of the stress tensor
σ_{ij} *[*$\sigma_{ij} = \sigma_{ji}$ *(*$i \neq j$*);* $\sigma_{i3}=\sigma_{3i}=0$*]* [9,13] as:

$$\varepsilon_{\phi,\psi}^{hkl} = \frac{d_{\phi,\Psi}^{hkl} - d_0^{hkl}}{d_0^{hkl}} = S_1^{hkl}\left(\sigma_{11} + \sigma_{22}\right) + \frac{1}{2} S_2^{hkl} \sigma_\phi \sin^2 \psi \qquad (1)$$

with

$$\sigma_\phi = \sigma_{11} \cos^2 \phi + \sigma_{12} \sin 2\phi + \sigma_{22} \sin^2 \phi \qquad (2)$$

Where ψ is the angle between the normal to the diffracting set of lattice planes [hkl] and the normal to the specimen surface, ϕ is the rotation angle within the plane of the layer (see Figure 2). $d_{\phi,\psi}^{hkl}$ is

the lattice spacing of [hkl] planes in the direction defined by ϕ and ψ, and d_0^{hkl} is the corresponding strain-free lattice spacing of [hkl] planes. S_1^{hkl} and S_2^{hkl} are elastic constants for lattice plane [hkl]. For a polycrystalline specimen with random crystallite orientation and a negligible variation of σ_{ij} over the depth probed, $\varepsilon_{\phi,\psi}^{hkl}$ depends linearly on $sin^2\psi$.

For the case of Mo, the direction used is [321]. The peak is found around the 2θ range 129-137 º.

2. Experimental

2.1. Film Deposition

Deposition of Mo was done by dc magnetron sputtering. The Mo target purity was N4 and it was used Ar N5 as the sputtering gas. Mo films were deposited on 3×3 cm^2 soda lime glass (SLG), which were cleaned with acetone, alcohol, hot deionised water and dried using a N_2 flux. The base pressure of the chamber was 5×10^{-6} mbar. Thicknesses were monitored with a quartz crystal monitor Intellemetrics IL 150. The working pressure in the chamber could be changed in the interval of $1x10^{-3}$ and $1x10^{-2}$ mbar. This was done by changing the Ar flow or by opening a butterfly valve. In this study we have always used the same flow of Ar to calibrate the butterfly position at a predefined pressure. Pressure then could be changed using different Ar flow values. It was used a sputtering power density of 0.5W/cm^2 and the substrate-to-target distance was 10 cm.

2.2. Film Characterization

Several methods have been used to characterize the films. Four Point Probe was used to measure the Sheet Resistance of the films; a Dektak 150 step profiler was used to measure film thicknesses; reflectivity was measured using a double beam Shimadzu spectrophotometer UV-3600; films' adhesion was tested by the Scotch tape test [10] and the rocking curve method was used to calculate the stress state of the films, finally XRD analysis were used to see the preferential orientation of the Mo films. X-ray diffraction (XRD) was done with a PHILIPS PW 3710 with a Cu-Kα line of 1.5406 Å. Scanning electron microscopy (SEM) was used to see the morphology of the sample and a Hitachi SU-70 with a acceleration voltage of 7 kV was used.

It was considered that the Scotch tape test or adhesion test had only two results, good or bad. If after the application of the tape the film was not damaged, then the adhesion was good, otherwise it was considered bad.

2.2.1. Resistivity

As stated before, the four point probe method was used to measure the sheet resistance (ρ_s) of the films. Knowing the sheet resistance and the thickness (h) of the films it is possible to estimate the resistivity (ρ) using the following equation:

$$\rho = h \cdot \rho_s \tag{3}$$

This equation is valid for square uniform samples.

2.2.2. Rocking Curves

For these measurements a x-ray diffractometter with a CuK_α radiation was used. For measuring the profiles of the Mo [321] peak, a scan between 0º and 63º in the ψ direction was done. It was used Bragg's Law to calculate $d^{321}_{\phi,\Psi}$. The curves were fitted using a Voigt function.

By using the slope of $d^{321}_{\phi,\Psi}(sin^2\psi)$ and equation 1 it is possible to estimate the value $\frac{1}{2}S_2^{321}\sigma_\phi$. The linearization was done in the interval of 0.25 to 0.7 $\sin^2\psi$. S_2^{321} takes the value of 4.76×10^{-6} MPa^{-1} [9,10] and therefore it is possible to calculate σ_ϕ. Although, it is also possible to determine bi-axial components of the stress tensor, since these follow the general behaviour of σ_ϕ, this component is enough to evaluate the stress state of the films.

3. Results and Discussions

3.1. Single layer films

Single layer Mo films were initially deposited to test the different regimes described by Scofield *et al* [11] and analyse the reproducibility of such conditions in our chamber. In table 2 the results of the first experiments are shown. For this set of experiments the main purpose was to identify the changes in adhesion and resistivity as function of the pressure.

Table 2 shows the same tendency that has been reported by Scofield *et al* [10] for all properties. Films sputtered at high pressure have good adhesion and bad resistivity and films at lower pressure have the opposite properties. In figure 2 it is possible to see the resistivity as function of the pressure. The results follow the same tendency as shown in previous studies [9, 10].

Table 2. Properties of single layer Mo films.

Pressure (mbar)	Adhesion	Resistivity (μΩ.cm)
$10x10^{-3}$	Good	411.0
$6x10^{-3}$	Good	330.4
$4x10^{-3}$	Bad	82.7
$1x10^{-3}$	Bad	36.3

From these results it is evident that there are two regimes when depositing Mo. The first regime, at pressures between $6x10^{-3}$ and $10x10^{-3}$ mbar, produces samples with good adhesion but with a high resistivity. In the second regime, at pressures between $4x10^{-3}$ and $1x10^{-3}$ mbar, the samples have bad adhesion but a lower resistivity as it is shown in Figure 2.

This analysis demonstrates what regimes we can use to do the bi-layer. The first layer should be deposited in a pressure higher than $6x10^{-3}$ mbar to obtain good adhesion and the second with a pressure smaller then $4x10^{-3}$ mbar to obtain a low resistivity.

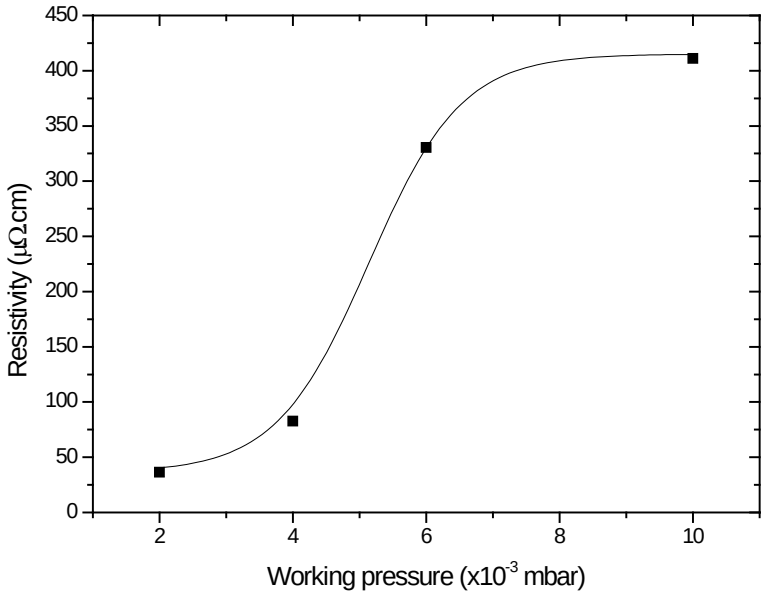

Figure 2: Mo film resistivity versus working pressure.

3.2. Bi-layer films

For this test it was decided to deposit a layer at high pressure at the bottom followed by a layer at low pressure at the top. It was decided to make the bottom layer with 500 nm and to study the variation of the thickness of the top layer. The pressures chosen were $10x10^{-3}$ mbar for to the bottom layer and $4x10^{-3}$ mbar for to the top layer. Between the two different pressures there is a period of 2 minutes. During this time the pressure is lowered in 1 minute and the tooling factor is changed in the other minute. Since this is not automatic these transitions are different from film to film and can change the final thickness of the film.

Table 3: Description of the bi-layer process with $10x10^{-3}/4x10^{-3}$ mbar.

Sample	Step	Pressure (mbar)	Monitor Thickness (nm)	Total measured thickness (nm)	Adhesion	ρ_s ($\Omega_{\square}$)	ρ ($\mu\Omega$.cm)
1	1	$10x10^{-3}$	500	685	Good	4.5	307.68
	2	$4x10^{-3}$	200				
2	1	$10x10^{-3}$	500	808	Good	2.4	194.07
	2	$4x10^{-3}$	300				
3	1	$10x10^{-3}$	500	911	Bad	1.8	163.98
	2	$4x10^{-3}$	400				

By looking at the properties presented in Table 3, we see that when the top layer is thin, then the film properties are close to those of the single layer samples deposited at high pressure. In the other extreme case, where the top layer is as thick as the bottom layer, the film has bad adhesion and the lowest resistivity. The best sample of this run was the one in which the bottom layer had 500 nm and the top layer had 300 nm. For the top layer of 400 nm there was poor adhesion and so continuing to increase the thickness of the top layer was useless. The value of 1.8 $\Omega\square$ for the sheet resistance is not low enough and therefore the deposition pressure of the top layer was further decreased.

In Table 4 the properties of the Mo films with a top layer deposited at $1x10^{-3}$ mbar are presented. Four different second layers were used, 50 nm, 200 nm, 300 nm and 450 nm. This time with increasing thickness of the top layer no noticeable degradation in the adhesion was observed. In the case in which the top layer had 450 nm it was noticed a degradation in the value of the resistivity as shown in Figure 3. This was supposedly due to a worse adhesion but the test was not able to confirm it.

Table 4: Parameters and results of the bi-layer deposition with $10x10^{-3}/1x10^{-3}$ mbar pressures.

Sample	Step	Pressure (mbar)	Controller Thickness (nm)	Adhesion	Total measurement thickness (nm)	ρ_s ($\Omega_{\square}$)	ρ ($\mu\Omega$.cm)
1	1	$10x10^{-3}$	500	Good	567	1.6	90.7
	2	$1x10^{-3}$	50				
2	1	$10x10^{-3}$	500	Good	717	0.8	57.4
	2	$1x10^{-3}$	200				
3	1	$10x10^{-3}$	500	Good	817	0.6	49.1
	2	$1x10^{-3}$	300				
4	1	$10x10^{-3}$	500	Good	972	0.8	77.8
	2	$1x10^{-3}$	450				

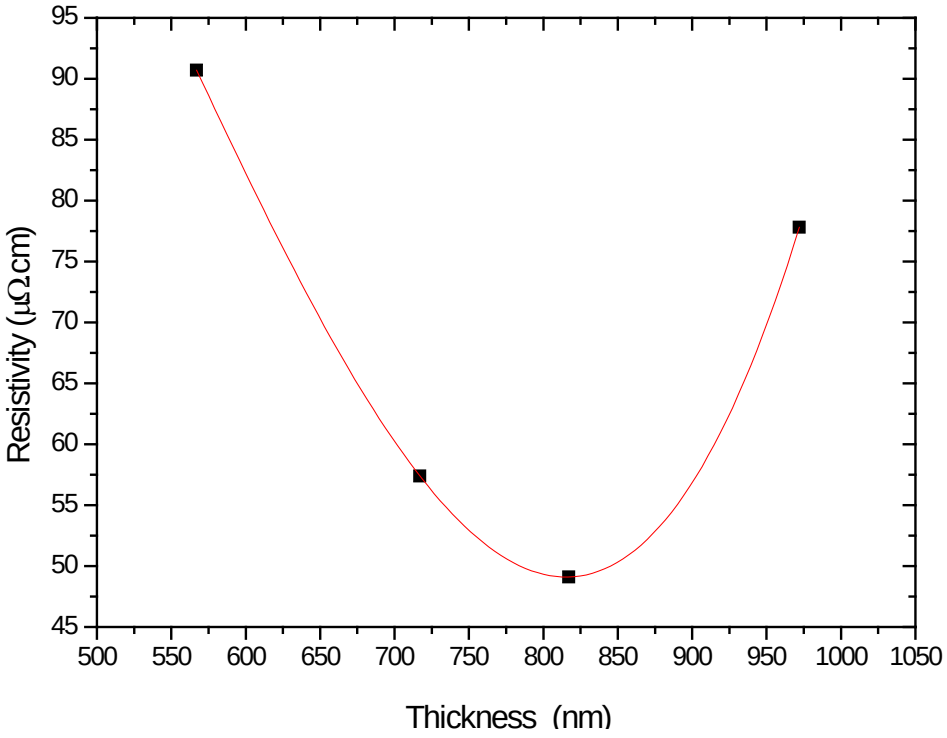

Figure 3: Resistivity versus thickness for samples deposited at with a bottom layer of 500 nm deposited at $10x10^{-3}$ mbar and different top layers deposited at $1x10^{-3}$ mbar.

Sample number 3 presented the lowest resistivity and had a good adhesion. This sample showed a sheet resistance of 0.6 Ω□ with a total thickness of 817 nm which corresponds to a resistivity of 49.1 μΩ.cm. This value of resistivity is very close to that of a Mo single layer deposited at $1x10^{-3}$ mbar. There are some differences between the monitored thicknesses and the ones measured with the profiler but these differences are small and acceptable.

Since it was shown for these pressure ranges that the lowest achievable resistivity was 49.1 μΩcm for the sample with thickness 500+300 nm at $10x10^{-3}$ /$1x10^{-3}$ mbar, it was decided to study further samples deposited in these conditions.

4. Characterization of the bi-layer films

An important question that has arisen from the last test was the reproducibility. Since there was a difference between the crystal monitor values and the measured thickness values it was important to check if this error was systematic or random. To investigate this problem, several samples were deposited. This was done for more than 4 runs, each with 4 films. It was then noticed that all the films had good adhesion. Their thicknesses were between 800-900 nm and the sheet resistance values were between 0.5 and 0.8 Ω□. These differences were most likely due to the pressure transition time between the bottom and top layers. This transition was done manually and therefore variations may exist from sample to sample.

To ensure that the film could resist the temperature of growth of CIGS, one of the samples was placed in the deposition chamber and heated up to 580 ºC for one hour. The Mo film was able to sustain these high temperatures.

The XRD spectrum presented in Figure 4 shows the typical cubic Mo structure with the following visible peaks: (110) direction with a peak at 40.46 º and d_{110} = 2.22 Å and a small peak at 73.75 º which corresponds to the (221) direction with d_{221} = 1.28 Å. The peaks of the (220) reflection at 87 º and (310) at 101 º are very weak. Using Scherrer's formula for the (110) direction, it was estimated that the crystallite size is about 40 nm. This is bigger then the grain size of 10 nm reported by Vink [9]. The lattice parameter, *a*, was estimated to be 3.13 Å against the 3.10 Å predicted by the XRD database [14]. This variation is smaller then 1% and it is probably due to measurement errors.

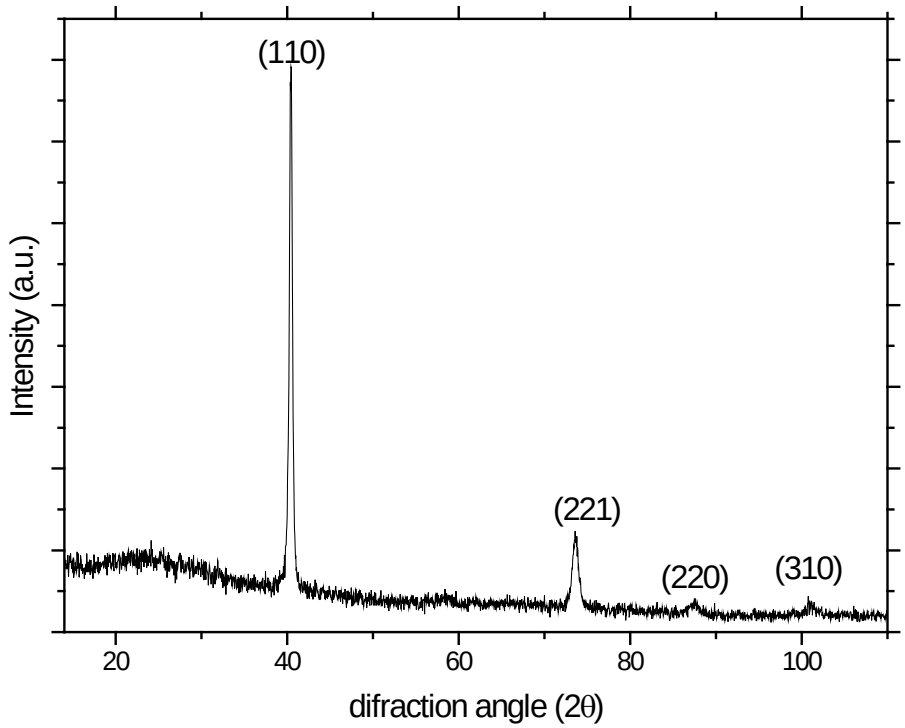

Figure 4. XRD spectrum of a Mo bi-layer film.

The stress calculations were made for a bi-layer film. In figure 5 a) it is presented the Voigt fit for a XRD measurement with ψ=35,84º. In Figure 5 b) it is plotted $d_{\phi,\Psi}^{321}$ versus the $\sin^2\psi$. Calculations of the stress tensor, σ_ϕ, were made as previously explained.

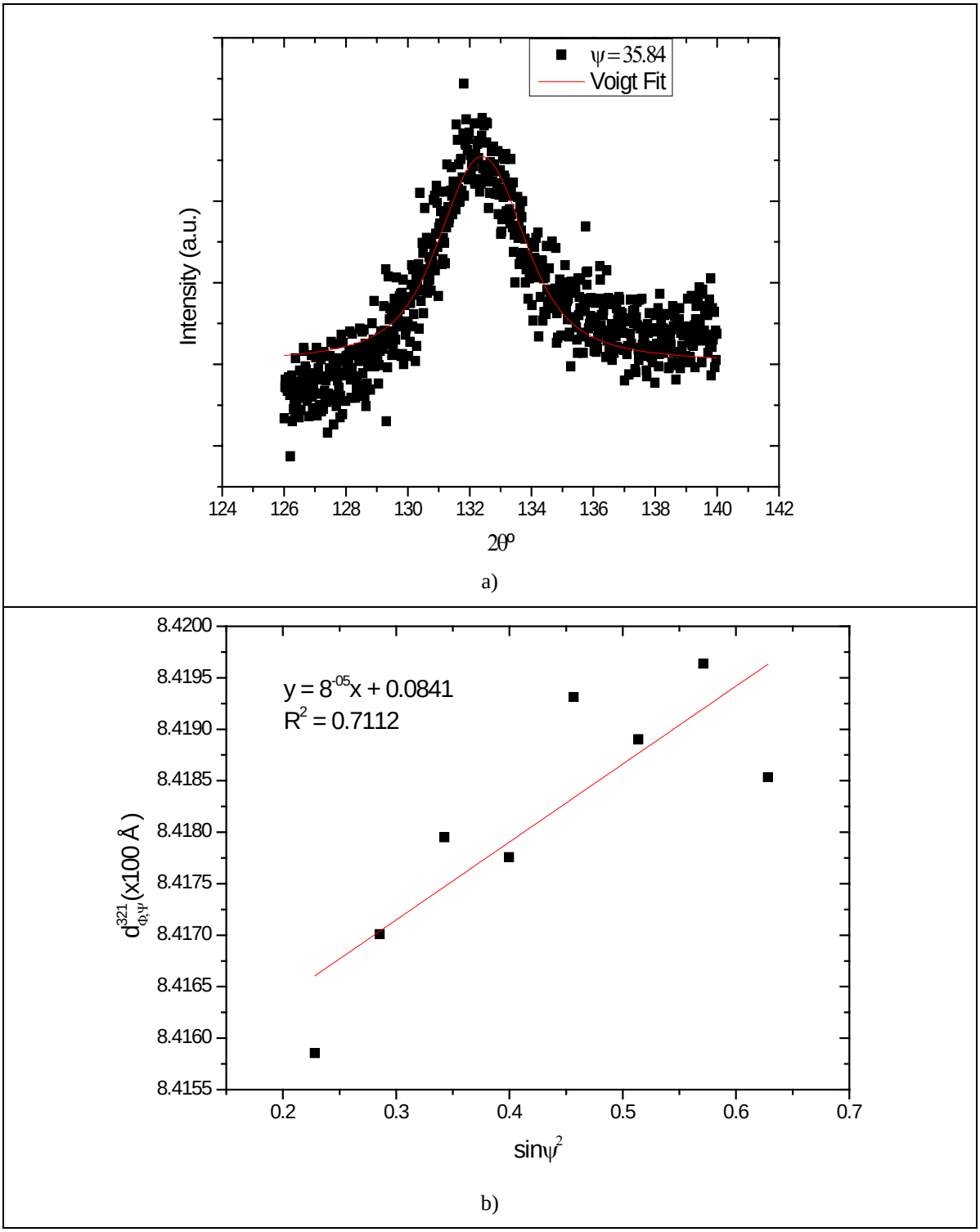

Figure 5: a) Example of Voigt fitting for ψ=35,84; b) $d^{321}_{\phi,\Psi}$ versus $sin^2\psi$ for a bi-layer Mo film.

As shown in Figure 5 b), not only the correlation between the points is low, but the slope of the curve is also low. Although the correlation is weak (R^2 of 0.7), it is evident that there is a general tendency for higher values of $d^{321}_{\phi,\Psi}$ with the increase of $\sin^2\psi$.This means that the film is in

a tensile state. The result of the stress tensor component, σ_{ϕ}, is 17 MPa, which is a low value. For comparison purposes, the values found by Vink *et al* [9] were in the order of GPa. This difference is possibly due to the fact that the film is too thick, but it is also possible that this is a mean value for a film with the top half in a compressive state and the bottom half in a tensile state. Nevertheless the important film properties had the desirable values.

In figure 6, a SEM image of the cross section of a Mo bi-layer is presented. The film shows a columnar growth and it is possible to see the bottom layer with 500nm and the top layer with 300 nm.

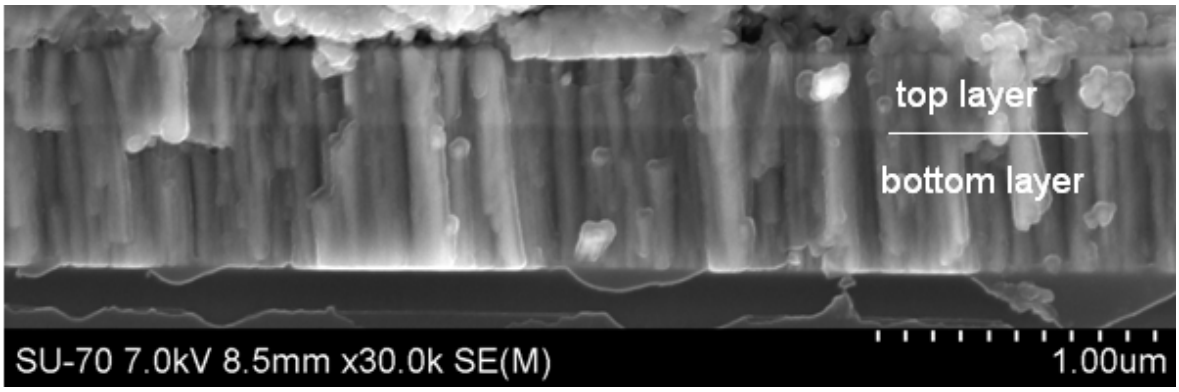

Figure 6: SEM image of the cross section of a Mo-bilayer.

5. Conclusions and Outlook

The main goal of this work was to clearly identify the deposition conditions, lacking in the literature, that ensured the deposition of Mo bi-layers with good adhesion to the SLG, a sheet resistivity lower than 1 Ω□ and good reproducibility of the former two properties. In this paper we presented the results of a study for varying pressure and thickness of the top layer. A detailed study of the resulting bi-layers was made, and the optimal result was achieved when the bottom layer was deposited at $10x10^{-3}$ mbar with a thickness of 500 nm and the top layer deposited at $1x10^{-3}$ mbar with a thickness of 300 nm. The bi-layers produced by this method meet the desired properties by having a good adhesion and a sheet resistivity between 0.5 and 0.8 Ω□.

The resulting bi-layers were analysed and XRD studies showed a film with the typical Mo cubic structure and a crystallite size of 40 nm. Stress calculations showed that these films were in a low tensile state. These calculations were difficult to make due to the big dispersion of the data when analysing the rocking curves itself. The method proved to be reproducible and the films could withstand the harsh growth conditions of CIGS.

Acknowledgments

P.M.P. Salomé acknowledges the financial support of Fundação para a Ciência e Tecnologia (FCT), through a PhD grant number SFRH/BD/29881/2006. P. A. Fernandes thanks the financial support of the FCT, through a PhD grant number SFRH/BD/49220/2008. The national network of microscopy is acknowledged: FCT: REDE/1509/RME/2005.

The authors also acknowledge Eng.ª Rosario Soares for the rocking curves measurements.

References

[1] N.G. Dhere, *Solar Energy Materials & Solar Cells*, **91**, 2007, 1376–1382.

[2] M. A. Green, *Prog. Photovolt: Res. Appl.*,**14**, 2006, 383–392.

[3] Rudmann, Dominik, "Effects of sodium on growth and properties of Cu(In,Ga)Se2 thin films and solar cells"; *DISS. ET*, Nr. 15576, 2004.

[4] L. Assmann, J.C. Bernède, A. Drici, C. Amory, E. Halgand, M. Morsli, *Applied Surface Science*, **246**, 2005, 159–166.

[5] T. Wada, N. Koharab, S. Nishiwaki, T. Negami, *Thin Solid Films*, **387**, 2001, 118-122.

[6] H.S. Ullal and B. von Roeder, *Solid State Technology*,2008, 52-54.

[7] A. Čampa, J.Krč, J. Malmström b, M. Edoff, F. Smole, M. Topič, *Thin Solid Films*, **515**, 2007, 5968–5972.

[8] K. Orgassa, H.W. Schock, J.H. Werner, *Thin Solid Films*, **431**, 2003, 387–391.

[9] T. J. Vink, M. A. J. Somers, J. L. C. Daams and A. G. Dirks, *J. Appl. Phys.*, **70** (a), 1991, 4301-4308.

[10] John H. Scofield,, A. Duda, D. Albin, B.L. Ballard, P.K. Predecki, *Thin solid Films*, **260**, 1995, 26-31.

[11] Jonh A. Thorton, Joseh E. Greene; Sputter deposition Processes in Handbook of Deposition Technologies for films and coatings; Roitan F Bunshah; *Noyes Publications*, *Second Edition*, New Jersey, 1994.

[12] Mattox, D.M ; Handbook of Physical Vapor Deposition (PVD) Processing; *William Andrew Publishing/Noyes*, 1998.

[13] U. Welzel, J. Ligot, P. Lamparter, A. C. Vermeulen and E. J. Mittemeijer, *J. Appl. Cryst.* (2005). **38**, 1–29

[14] ICVD 04-001-2734.